Scientia Iranica B (2018) 25(4), 2087–2097

SCIENTIA IRANICA

Sharif University of Technology
**Scientia Iranica**
*Transactions B: Mechanical Engineering*
http://scientiairanica.sharif.edu

# Analysis of nonlinear acoustic wave propagation in HIFU treatment using Westervelt equation

**S. Haddadi[a] and M.T. Ahmadian[b,*]**

a. *School of Mechanical Engineering, Sharif University of Technology, Azadi Ave., Tehran, Iran.*
b. *Center of Excellence in Design, Robotics and Automation (CEDRA), School of Mechanical Engineering, Sharif University of Technology, Tehran, P.O. Box 11155-9567, Iran.*

Received 18 July 2016; received in revised form 8 March 2017; accepted 10 June 2017

**KEYWORDS**
HIFU;
Nonlinear wave propagation;
Pennes's bio-heat equation;
KZK equation;
Westervelt equation.

**Abstract.** Currently, the HIFU (High-Intensity Focused Ultrasound) therapy method is known as one of the most advanced surgical techniques of tumor ablation therapy. Simulation of the non-linear acoustic wave and tissue interaction is essential in HIFU planning to improve the usefulness and efficiency of treatment. In this paper, linear, thermoviscous, and nonlinear equations are applied using two different media: liver and water. Transducer power of 8.3-134 Watts with the frequency of 1.1 MHz is considered as the range of study to analyze the interaction of wave and tissue. Results indicate that the maximum focal pressure of about 0.5-4.3 MPa can be achieved for transducer power rates of 8.3 to 134 W. The simultaneous solving of the acoustic pressure and Pennes's bio-heat equations can help determine the amount of temperature rise at the focal point and ablated area. Finally, the linear and nonlinear simulations are compared, and the turning point of transition from linearity to nonlinearity is determined. The simulated results provide us with the required information about the behavior of the focalized ultrasound in interaction with liver tissue. The performance of phased array HIFU transducer can be improved for treatment considering lesion size as well as temperature rise in tissue and for choosing the best range of operational power.



## 1. Introduction

Cancer has been one of the main reasons of death in the last decades all around the world. Nowadays, many solid cancerous cells in various parts of the body, including pancreas, prostate, breast, uterine fibroids, and liver, are eroded by High-Intensity Focused Ultrasound (HIFU) radiation as one of the efficient emerging medical therapies [1,2]. In comparison with other conventional cancer treatment techniques, such as surgery, radio- and chemo-therapy, HIFU has the advantage of being non-invasive without ionization; besides, less post-treatment requirements are reported [3]. However, severe side effects may occur during the therapy if the vital blood vessels around the tumors are subjected to damage by HIFU Hynynen et al. [4]. Understanding the HIFU process makes it possible to control and save the desired treatment area from failure and to assure the safety of patients and effectiveness of the treatment.

With the advent of the computers, which have the ability to solve wave equations numerically, studying the effects of nonlinear wave propagation in different media has become possible Bjorno [5]. Wave propagation is a nonlinear phenomenon, especially in tissue and human organs. Therefore, assuming a linear wave

*. *Corresponding author. Tel: +98 21 66165503*
*E-mail addresses: s_haddadi@mech.sharif.edu (S. Haddadi); ahmadian@sharif.edu (M.T. Ahmadian)*

doi: 10.24200/sci.2017.4496

equation, especially with high-amplitude, does not give a correct solution to wave propagation problem. Many efforts have been made to better predict the effects of nonlinearities on the wave propagation, making it an interesting field of study for many researchers in order to determine and investigate the nonlinear behaviors of waves [3,6-8].

There are many different methods for solving nonlinear wave equations, each with advantages and disadvantages. Implementation of different numerical methods in modeling can predict system behavior with different accuracies. The most common method for solving wave equations is the Finite-Difference Method (FDM). Okita et al. [9] used the FDM to simulate the HIFU waves on brain tumors. The Finite-Element Method (FEM) is another way to simulate the wave equation with good accuracy. Wong et al. [10] applied the FEM to the simulation of CMUTs. An extensive set of issues in mechanical engineering, especially in the field of biomechanics, can be usually solved by the FEM method. In the HIFU simulation, the FEM can calculate the ablation area in an efficient way based on the transducer power, tissue type, and exposure time.

To date, many equations for simulating nonlinear wave propagation have been presented. Burgers equation in 1948, Westervelt equation in 1963, and KZK equation in 1971 Hamilton [11] are the most widely used equations to predict the propagation of nonlinear waves. The KZK equation usually gives an acceptable answer in simulated waves for transducers with aperture angles of less than 18 degrees [12,13]. The good choice of boundary condition in KZK equation may extend its area of application. However, to simulate the wave propagation for transducers with aperture angles of more than 18 degrees, the Westervelt equation is generally used [14,15].

The subject of how best to model the physical interactions between ultrasound waves and biological tissue has been widely considered, and investigations in this area are still making progress. At high intensities, nonlinear wave propagation effects lead to the distortion of the waveform. Higher harmonics are generated due to the nonlinear distortion. The tissue, while enhancing the local heating, more readily absorbs higher harmonics. The peak temperature at focus predicted by a nonlinear equation field is markedly higher than that predicted by a linear equation due to strong absorption of the higher-frequency harmonics.

At low focal intensities, nonlinear effects cause energy to be generated up to at least the 10th harmonic [16]. At very high focal intensities where strongly shocked waves are produced, as many as 600 harmonics might be required to model the focal heating accurately [17]. Thus, the frequency content of the propagating ultrasound waves can be very broadband. Solving large problems involving high focal intensities is still a big challenge.

In the present study, a HIFU transducer that is spherically focused with an aperture angle of maximum 30 degrees and a focal length of 50 mm is used. Wave interaction with the liver tissue is simulated in four points in the range of 8.3-134 W as the transducer power. Any increase in the transducer power and, consequently, pressure intensity leads to an intensification of the nonlinear effects. Therefore, the nonlinearity is considered in the numerical simulation. Numerical simulations can improve the prediction accuracy and increase the efficiency of the models in different case studies. Herein, HIFU wave propagation in both lossless and thermoviscous media is simulated, and the effects of the nonlinear factors in different pressures on wave propagation are studied.

## 2. Methods

### *2.1. Numerical method*

To study the HIFU treatment, ultrasound wave propagation across a heterogeneous medium, such as a liver, should be explained. Two PDEs for acoustic wave propagation and biological heat transfer are simultaneously solved in the liver medium. The acoustic equation in the wave propagation problem can be generally divided into three different types. The first one is a linear wave equation for simulating waves with a low energy level and short amplitude in a lossless medium. The second type is studying the effects of thermal conductivity and viscosity on the equation. This type of equation leads to a satisfactory answer for media with high loss. Finally, to simulate wave propagation by considering the effects of high amplitude and energy dissipation in heterogeneous environments, the best answer comes from solving the nonlinear equations. Herein, in order to evaluate and compare different wave propagation types, equations should be solved in the time domain.

#### *2.1.1. Linear acoustic wave equation*

In solving the linear acoustic wave equation, the medium is assumed to be lossless. The linear wave equation used in Comsol software (Comsol Multiphysics® version 5.1, Comsol Company, Sweden) is Eq. (1). This equation in the time domain (transition state) can be expressed as follows:

$$\frac{1}{\rho c^2}\frac{\partial^2 p_t}{\partial t^2} + \nabla . \left(-\frac{1}{\rho_c}(\nabla p_t - q_d)\right) = Q_m, \tag{1}$$

$$p_t = p + p_b, \tag{2}$$

where $p$ is the pressure, $c$ is the speed of sound, $t$ is the time, and $\rho$ is the density. In addition, $Q_m$ and $q_d$ are the monopole and dipole terms, respectively, and are defined in the software separately. In this equation, attenuation can be defined in the monopole term as a source. The linear equation is derived from inputting the value of $Q_m = q_d = 0$.

*2.1.2. Thermoviscous wave equation*

The thermoviscous equation in Comsol software is as follows:

$$\frac{1}{\rho c^2}\frac{\partial^2 p_t}{\partial t^2} + \nabla.\left(-\frac{1}{\rho_c}(\nabla p_t - q_d) + \frac{1}{\rho c^2}\left(\frac{4\mu}{3} + \mu_B + \frac{(\gamma-1)k}{C_p}\right)\frac{\partial \nabla p_t}{\partial t}\right) = Q_m, \tag{3}$$

where $\mu$ is the viscosity, $C_p$ is the heat capacity, $\gamma$ is the ratio of specific heats, and $k$ is the thermal conductivity.

This equation for the media with high-energy loss has acceptable accuracy. The term $(\frac{4\mu}{3} + \mu_B)$ in the equation is related to the viscosity, showing that the losses are enhanced in higher viscosity. This means that as the medium gets nearer to gas phase, the influence of the viscosity reduces. Another term is $(\frac{(\gamma-1)k}{C_p})$, which studies the effects of the thermal conductivity. By going from the gas phase to the solid phase, the compressibility factor will decrease and $C_p$ value will be equal to $C_v$. Therefore, reducing the compressibility decreases the impact of the thermal conductivity. In addition, in the thermoviscous simulation, the values of $Q_m$ and $q_d$ are zero.

*2.1.3. Acoustic nonlinear equation*

A nonlinear acoustic field can be simulated by Eq. (4); this equation is known as the Westervelt equation and can be used to simulate acoustic pressure in tissue:

$$\nabla^2 p - \frac{1}{c_0^2}\frac{\partial^2 p}{\partial t^2} + \frac{\delta}{c_0^4}\frac{\partial^3 p}{\partial t^3} = -\frac{\beta}{\rho_0 c_0^4}\frac{\partial^2 p^2}{\partial t^2}, \tag{4}$$

where $p$ is the acoustic pressure, $\beta = 1 + B/2A$ is a nonlinearity coefficient, and $\delta$ is the diffusivity of sound, which comes from viscosity and thermal conductivity. The value of $\delta$ can be calculated from Eq. (5):

$$\delta = \frac{1}{\rho_0}\left(\frac{4\mu}{3} + \mu_B\right) + \frac{k}{\rho_0}\left(\frac{1}{C_v} - \frac{1}{C_p}\right). \tag{5}$$

The first and second terms of Eq. (4) represent a linear propagation of waves in a medium without any loss. The third term is related to the losses due to the thermal conductivity and viscosity of the fluid. The last term of the equation is related to the nonlinear factors influencing the simulation of wave propagation and causing thermal and mechanical changes within the tissue.

Nonlinear propagation of sound beam in a thermovisous fluid may also be described by the KZK equation [11]:

$$\frac{\partial^2 p}{\partial z \partial t_{KZK}} = \frac{c_0}{2}\nabla^2 p + \frac{\delta}{2c_0^3}\frac{\partial^3 p}{\partial t_{KZK}^3} + \frac{\beta}{2\rho_0 c_0^3}\frac{\partial^2 p^2}{\partial t_{KZK}^2}. \tag{6}$$

To validate the proposed algorithm, harmonics generated by the concave transducer in a two-layer medium using the Comsol software are compared with those simulated using the KZK model (HIFU Simulator v1.2, Food and Drug Administration, Silver Spring, MD) [18].

To study the impact of nonlinear factors, both linear and nonlinear equations are calculated. Another important parameter in the simulation is the wave intensity. The intensity of the wave can be calculated by Eq. (7):

$$I = \frac{P_t^2}{2\rho_c}. \tag{7}$$

*2.1.4. Bio-heat transfer equation*

The heat generated anywhere in the tissue is affected by two important parameters. The first parameter is the acoustic wave adsorption coefficient as one of the intrinsic properties of the tissue, and the second is the sound wave intensity, calculated by solving the wave equation on the tissue geometry of the study. Therefore, the heat source can be achieved by Eq. (8):

$$Q = 2\alpha_{\text{abs}} I. \tag{8}$$

In the above equation, $\alpha_{\text{abs}}$ is the attenuation coefficient, which is proportional to the frequency and calculated by Eq. (9):

$$\alpha = \alpha_0 \left(\frac{f}{f_0}\right)^{\eta}. \tag{9}$$

$\alpha_0$ is the attenuation coefficient at the frequency of $f_0 = 1$ MHz and $\eta = 1$ in soft tissue.

The Westervelt equation is obtained for thermoviscous fluids. The attenuation in the thermoviscous fluids is proportional to Eq. (9). This relation is linear for a soft tissue [19].

Eq. (8) is considered a heat source of the heat transfer equation. Heat transfer is studied within the tissue in this simulation; therefore, the main mechanism of heat transfer and heating the tissue during wave propagation or afterward is the thermal conductivity. Therefore, the heat transfer equation can be written as in Eq. (10), which is dependent on time:

$$\rho C_p\left[\frac{\partial T}{\partial t} + (u.\nabla)T\right] = \nabla.(k\nabla T) + Q + Q_{\text{bio}}. \tag{10}$$

Considering that convection is not a governing heat transfer mechanism in this case, the second term on the left hand of Eq. (10) can be neglected. $Q_{\text{bio}}$ is calculated from Eq. (11):

$$Q_{\text{bio}} = \rho_b C_b \omega_b (T_b - T) + Q_{\text{met}}. \tag{11}$$

$T_b$ is the arterial blood temperature.

### 2.2. Thermal dose

The thermal dose, which is defined by Sapareto and Dewey [20], indicates the relation between the time and temperature to heat the tissue in order for necrosis to occur. In HIFU surgery (temperature is usually above 50°C), the thermal dose is defined as follows:

$$TD = \int_{t_0}^{t_{\text{final}}} R^{(T-43)} dt \approx \sum_{t_0}^{t_{\text{final}}} R^{(T-43)} \Delta T. \tag{12}$$

In Eq. (12), the values of $R$ for $T > 43$°C and $37°\text{C} < T < 43°\text{C}$ are equal to 2 and 4, respectively. According to this equation, if the tissue temperature increases to 43°C, the required time is approximately 240 minutes to reach cell death. If the temperature increases to 56°C, this time is reduced to 1 second.

### 2.3. Geometry

To solve the problem in a two-dimensional space, a transducer with a 50 mm length of the focal point and a hole in its center with a diameter of 10.22 mm (in order to reduce the occurrence of wave interference) is modelled. In this study, as shown in Figure 1, the tissue is immersed in a fluid medium (water). The tissue dimensions are 50 × 45 mm, and the propagation medium is assumed 120 × 120 mm.

### 2.4. Boundary conditions

In order to simulate wave propagation in a two-dimensional space, two sets of boundary conditions are needed. The first boundary condition is used for solving the acoustic equation and the second boundary condition for solving the heat transfer equation. The boundary conditions are defined as follows:

1. Boundary condition $P_t = P_0 \sin(\omega t)$ is used as the source pressure;
2. A plane wave radiation boundary condition is defined on the walls as a boundary condition without any reflection (transparent). The equation is:

$$-n.\left(-\frac{1}{\rho}(\nabla p_t - q_d)\right) + \frac{1}{\rho}\left(\frac{1}{c}\frac{\partial P}{\partial t}\right) = Q_i. \tag{13}$$

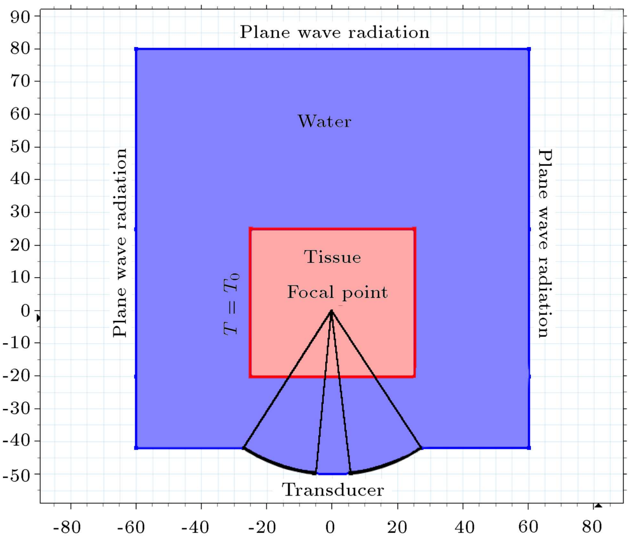


**Figure 1.** Geometry and boundary conditions used in the simulation.

3. The tissue wall boundary condition is defined as $T = T_0 = 310$ K.

The initial conditions for the acoustic equations are $P = 0$ and $\frac{\partial P}{\partial t} = 0$, and the initial condition for solving the heat transfer equation is $T = T_0 = 310$ K. Figure 1 shows the boundary conditions of the problem.

### 2.5. Problem description

In order to investigate the effects of nonlinearity on wave propagation, transducer surface pressures of 100, 200, 300, and 400 kPa are considered, which are equivalent to operating power rates of 8.3, 33.5, 75.4, and 134 W. The time step and total transient simulation time are 1 and 300 microseconds, respectively. After 300 microseconds, as a uniform pressure field is obtained, a steady-state acoustic pressure equation is considered to find the temperature distribution. Table 1 shows the parameters used in the simulation for water and liver tissue.

A frequency of 1.1 MHz is used in the simulation. The wave exposure time to determine the ablated area is 60 seconds.

At the focal point, an improved mesh size of $\lambda/8$ is used. Approaching the walls, the mesh size increases. A mesh dependency test is performed by reducing the mesh size by 30%, and the results indicate the changes of less than 1%.

**Table 1.** Parameters used in the simulation.

| | Attenuation Constant (1/m) | Density (kg/m$^3$) | Heat capacity (J/kg/°C) | Thermal conductivity (W/m/°C) | Speed of sound (m/s) | B/A |
|---|---|---|---|---|---|---|
| **Tissue (liver)** | 6.915 | 1078.75 | 3540 | 0.52 | 1586 | 6.8 |
| **Water** | 0.025 | 998.2071 | 4180 | 0.6 | 1482 | 5.2 |

## 3. Results

### 3.1. Model verification

In this article, model verification is based on experimental data extracted from the study by Karaböce and Durmuş [21] for temperature distribution, and the FDA HIFU simulator is used to verify pressure distribution.

HIFU Simulator is a freely distributed, MATLAB-based software package for simulating axisymmetric High-Intensity Focused Ultrasound (HIFU) beams [18] by employing KZK equation. The KZK equation has two main limitations, which do not exist in Westervelt equation. First, effects of reflection and scattering are not taken into account. Second, it can be applied only for the transducers with small aperture angles ($< 18°$).

HIFU Simulator is used to calculate the pressure at the focal point for transducer power rates of 33.5, 75.4, and 134 W. Results show that the deviations between Westervelt and KZK equations for transducer power rates of 33.5, 75.4, and 134 W are 10.6, 12.5, and 11.9 percent, respectively.

The large aperture angle is the main reason for the deviation between KZK and Westervelt nonlinear models.

### 3.2. One-dimensional wave simulation

It is essential to study the one-dimensional wave propagation characteristics to investigate the wave distribution and attenuation. For this purpose, one-dimensional simulations of the wave propagation along the water and liver tissue for nonlinear model are performed and represented in Figure 2. In these diagrams, the blue lines represent the wave propagation in the liver, and the black dashed lines display the propagation of waves in the water. These waves are generated by a monopole wave source with the ability of generating a sinusoidal wave with 200 kPa as the initial pressure.

In the magnified areas of a, b, and c, a phase lag of approximately $4\pi$ along the wave propagation direction can be seen. This is due to different speeds of sound in liver tissue and water. Furthermore, due to the higher viscosity of the liver, the amount of losses in the liver medium is more than water, which can be inferred from wave domain reduction along the longitudinal direction. Energy losses in the liver medium along the 50-mm path of wave propagation are more than approximately 28% of the water medium. This loss of energy mainly occurs due to the liver's higher viscosity. Inherent viscosity of the liver tissue causes shear force, while the ultrasound wave passes through it, converting some of the wave energy into the thermal energy.

It should be considered that diffraction and scattering properties of nonlinear model cannot be shown in one dimension, and these terms will be explained and clarified in a two-dimensional simulation.

### 3.3. Two-dimensional simulation

In the two-dimensional simulation, considering nonlinearity, thermoviscous terms, diffraction and scattering, and proper choice of acoustic pressure equation to obtain a precise answer aligned with the real experimental data is essential.

#### 3.3.1. Acoustic pressure field

The acoustic field in water and liver media produced

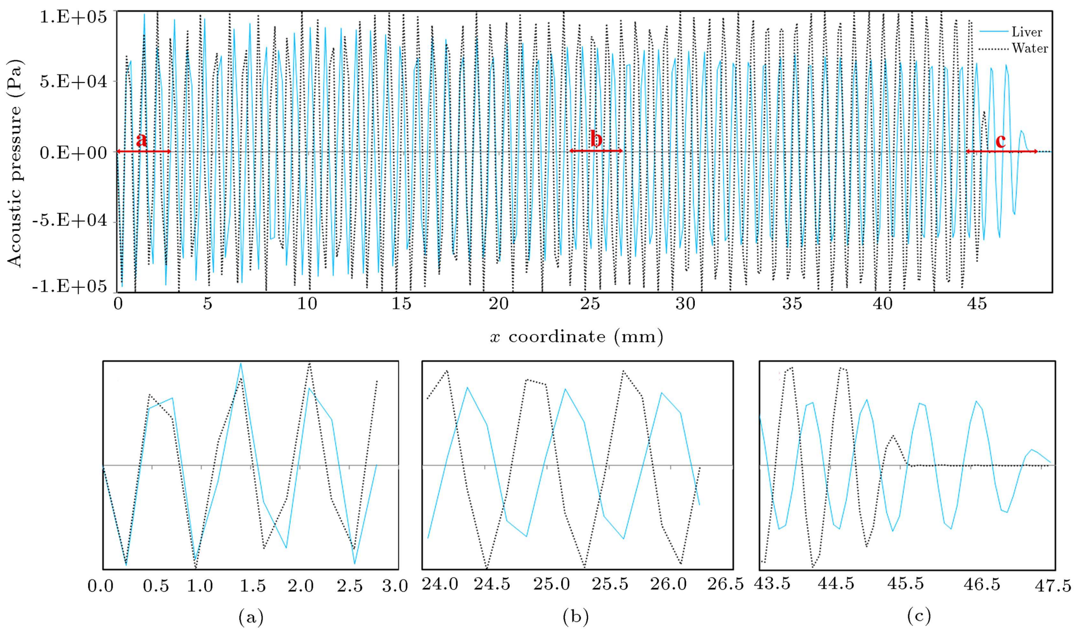


**Figure 2.** One-dimensional nonlinear wave propagation in liver and water versus distance: (a) 0-3 mm, (b) 24-26 mm, and (c) 43.5-47.5 mm from the transducer.

by the HIFU transducer with the power of 8.3-134 W is simulated that includes the transition range from linearity to nonlinearity.

### *3.3.2. The comparison of the linear and nonlinear acoustic pressure fields*

In this paper, Eq. (1) and the Westervelt equation are used for the numerical simulation of the linear and nonlinear wave propagations, respectively. Using the Comsol software, the thermoviscous and nonlinear parameters of the Westervelt equation are defined as monopole sources with time steps of 1 microsecond. Figure 3 shows the simulation results of the linear and nonlinear acoustic pressure equations after 50 microseconds radiation. The right picture shows the results of solving the linear pressure equation, while the left one shows the results of the nonlinear pressure equation.

Figure 4 shows the pressure variation along the lateral axis at the focal point. The transducer power is set to 134 W, and the maximum pressure at the focal point, as shown in Figure 4, for the nonlinear equation is equal to 4.3 MPa. According to this figure, the nonlinear curve is significantly affected by the excitation of higher harmonics, and the focal point shows a maximum pressure, which is 1.9 times greater than the maximum pressure in linear mode. Local maxima can also be seen in the nonlinear case that is due to superposition of waves with different wavelengths representing the higher harmonics.

The higher the pressure is, the more the nonlinear behavior of the wave increases. Figure 5 represents the nonlinear pressure curve for transducer power rates of 33.5, 75.4, and 134 W along the lateral-axis.

Figure 6 represents the acoustic pressure along the axial-axis. As shown in this figure, the nonlinear pressure is 1.9 times greater than the pressure in linear mode. In the thermoviscous case, a large part of the wave energy is lost because of the factors such as viscosity and specific heat rate that affect the wave and its absorption by the environment. Finally, this lost energy is absorbed and the tissue temperature is increased.

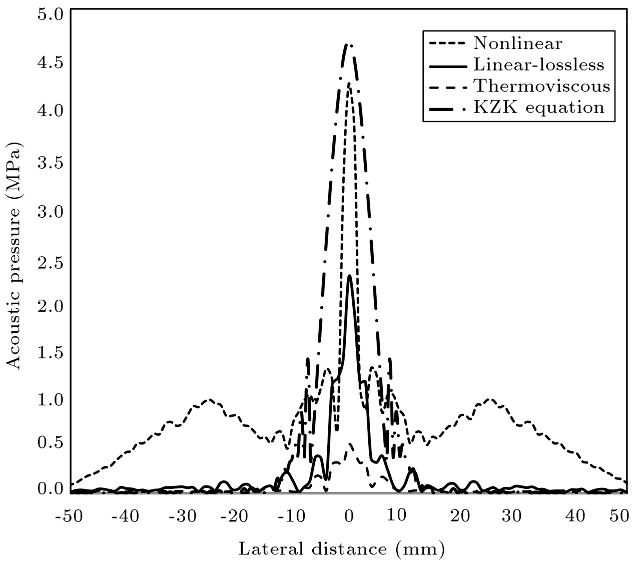


**Figure 4.** Pressure function along the lateral axis in the liver at the focal point. The operating power and frequency are 134 W and 1.1 MHz, respectively.

Figure 7 shows the acoustic pressure at the focal point for different powers. For powers greater than 40 W, the influence of nonlinear factors intensifies. In other words, the linear simulation assumption is not correct for powers greater than 40 W.

In the liver medium, at pressures higher than 4 MPa, the wave behavior is completely nonlinear, and the nonlinear simulation differs vastly from the linear assumption in this case. The ranges covering transducer power of 40-80 W and focal pressure of 1.5-2.5 MPa can be considered as the turning point for the

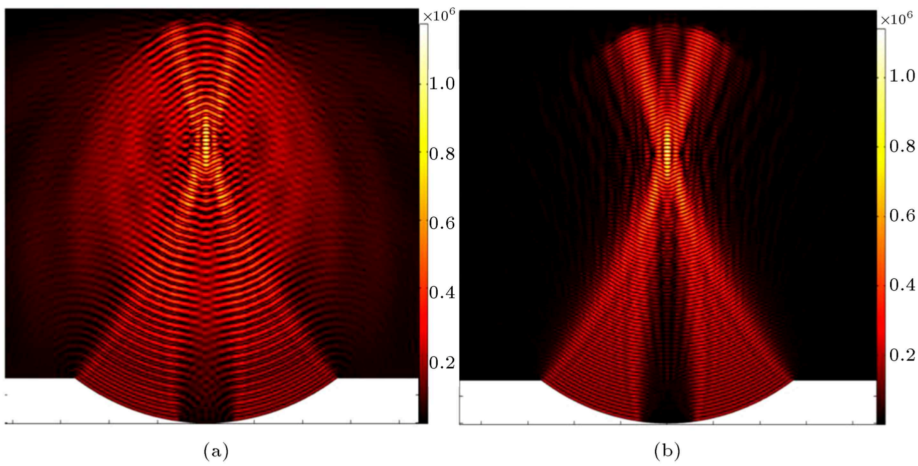


**Figure 3.** Acoustic pressure field results of the linear (a) and nonlinear (b) equations at radiation time of 50 microseconds in liver medium and 1.1 MHz as the wave frequency.

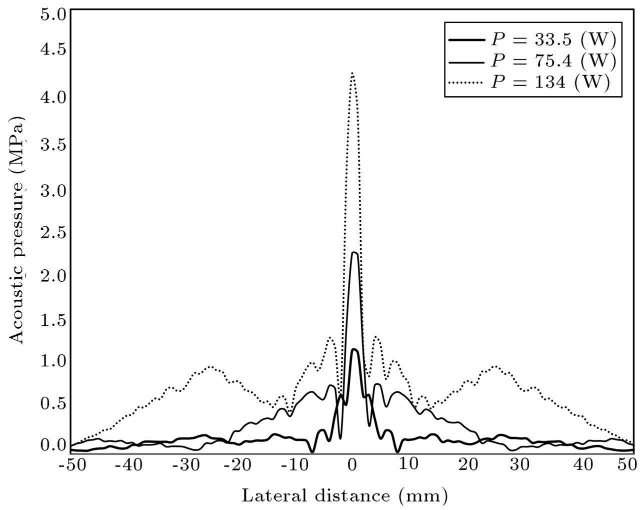


**Figure 5.** Nonlinear pressure curve in the liver for different operational powers along the lateral-axis across the focal point at 1.1 MHz frequency.

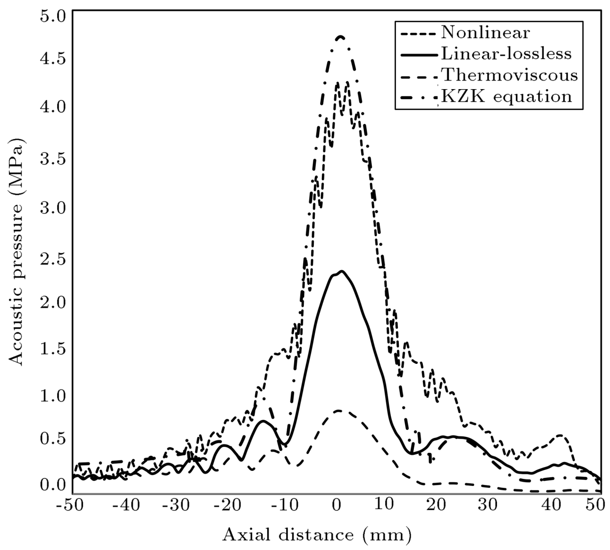


**Figure 6.** Acoustic pressure value for different equations along the axial-axis in the liver. Operating power and frequency are 134 W and 1.1 MHz, respectively.

transition from linear to nonlinear behavior in the liver tissue.

*3.3.3. The focal point temperature and ablated area*

The pressure at the focal point increases as the transducer power increases. This pressure rise leads to nonlinear behavior at the focal point, resulting in a sharp rise in the tissue temperature. Figure 8 shows the temperature increase and ablated area for different transducer powers. It can be concluded that the power increase and excitation of higher harmonics significantly influence the ablated area. Ablated area is calculated from thermal dose equation, and the results are shown in Figure 9.

Figure 10 shows the areas of the thermal dose

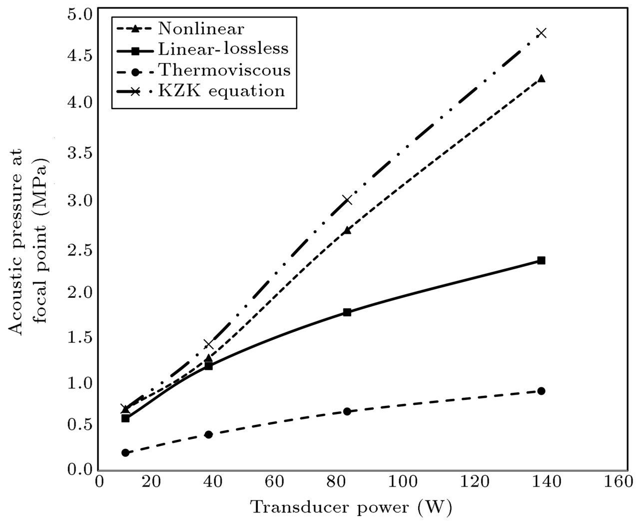


**Figure 7.** Acoustic pressure at the focal point in the liver versus different powers using linear, thermoviscous, and non-linear equations at 1.1 MHz frequency.

above the lethal threshold of 240 $CEM_{43}$. The Cumulative Equivalent Minutes at 43°C model ($CEM_{43}$), introduced by Sapareto and Dewey [20], represent the concept of thermal isoeffect dose: a reference temperature (43°C) has been chosen to convert all thermal exposures into equivalent minutes at this temperature.

It can be concluded from the results listed in Table 2 that, at higher powers, a smaller part of the tissue is affected by HIFU therapy; further, the required insonation time is much lower. Reduction of time and ablated area is of great benefit to surgeries in order to control the scope of damage to surrounding tissue. On the other hand, increasing the power and the focal pressure will extend the chance of cavitation occurrence, and the creation of micro-bubbles will spread the damage to neighbor tissues. Therefore, an optimum amount of power should be applied as the best solution, which is equal to the highest power possible before reaching the cavitation during operation on tissue.

In order to validate the temperature simulation, the ablated area related to radiation times of 5, 10, 15, ..., 40 seconds is calculated and compared with the experimental data from Karaböce [21]. The deviation between the predicted ablated area of the simulation and Karaböce's reported experimental results is calculated, implying that the two groups of data agree closely and the overall average error of less than 7% in terms of ablated area is observed.

## 4. Discussion

In this paper, Westervelt nonlinear equation is used to analyze the HIFU waves and tissue interaction. Two-dimensional analysis is performed in order to obtain the precise result for pressure distribution and attenuation

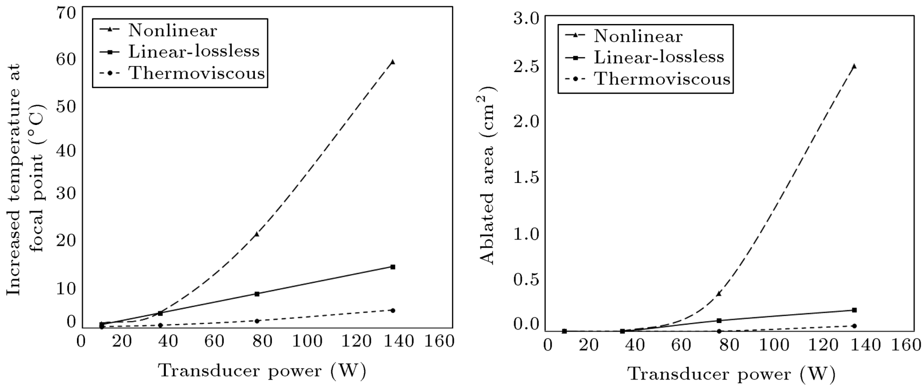


(a) (b)

**Figure 8.** (a) Increased temperature at the focal point in the liver by the application of different powers and exposure time of 60 s. (b) Ablated area at the focal point by the application of different powers and exposure time of 60 s.

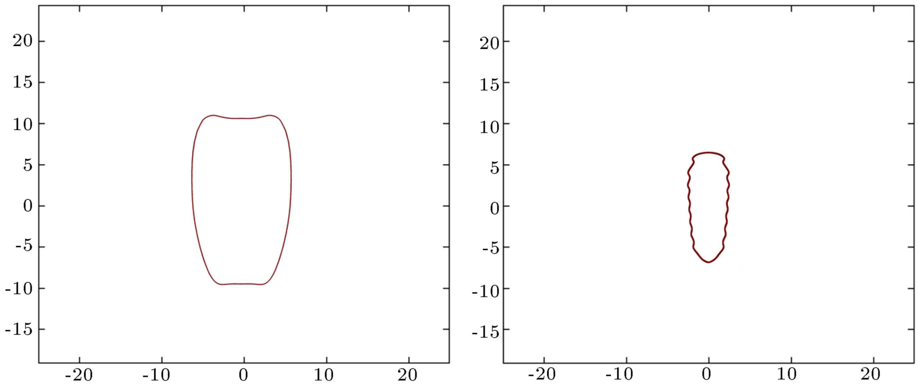

(a) (b)

**Figure 9.** Thermal dose contour and ablated area in the liver considering the exposure time of 60 s and 1.1 MHz frequency for (a) $P = 134$ W, and (b) $P = 75.4$ W.

**Table 2.** Ablated area results obtained for different transducer operating conditions in the liver and 1.1 MHz frequency.

| Case | Power (W) | Radiation time (s) | Ablated area (cm$^2$) |
|---|---|---|---|
| a | 134 | 8.3 | 0.12 |
| b | 75.4 | 35 | 0.30 |
| c | 33.5 | 660 | 1.88 |
| d | 8.3 | 1400 | 3.77 |

along the focal point. Linear, thermoviscous, and nonlinear Westervelt equations are applied by considering two different media: liver and water.

Considering the nonlinear effects, the acoustic pressure at the focal point is approximately 1.9 times higher than the linear result. The results show that the transient behavior ranging from complete linearity to nonlinearity happens in transducer power rates of 40-80 W. At powers more than 80 W, using the linear equation for analysis results in big differences in measured parameters and experimental findings; therefore, at high powers, it is necessary to consider the nonlinear terms in the equation.

Moreover, the application of higher pressures leads to a meaningful time reduction and reaching a desirable temperature to start cell death; this is beneficial to the achievement of a smaller, more controllable ablated area to prevent surrounding tissue damage. However, considering that higher power increases the probability of the cavitation phenomenon that makes controlling the surgical operating conditions difficult, an optimum operating pressure should be selected to have the best therapeutic effect.

In this study, it is shown that, using the transducer surface pressure of 400 kPa (equivalent to 134 W power), a 0.12 cm$^2$ ablated area can be achieved in 8.3 seconds. In this case, the tissue experiences a maximum focal pressure of about 4.3 MPa, which is

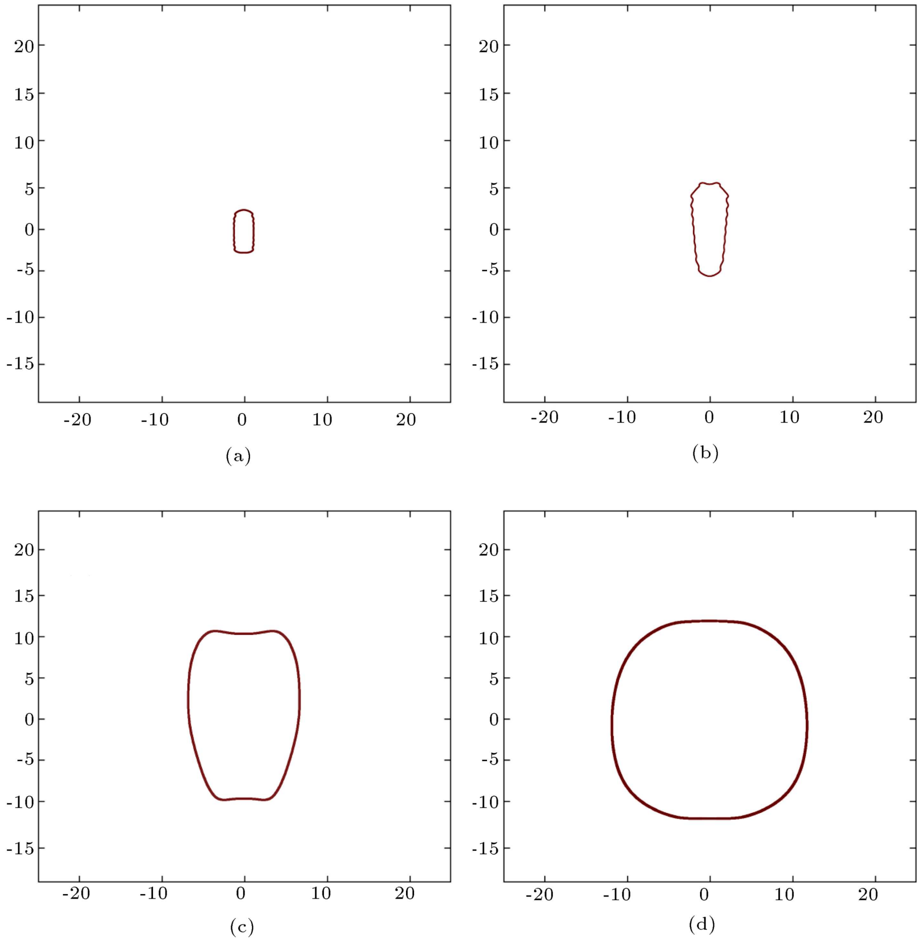


**Figure 10.** Amount of ablated area at the focal point in the liver and frequency of 1.1 MHz for various operational exposure times and powers of (a) 8.3 s and 134 W, (b) 35 s and 75.4 W, (c) 600 s and 33.5 W and (d) 1400 s and 8.3 W.

far enough from the 5.3 MPa threshold reported for the start of cavitation [22].

Cavitation is defined as the interactions between the ultrasound field and small bubbles containing gas. Usually, bubbles or small gas nuclei are naturally present in biological tissues; however, using HIFU will aid the creation and encapsulation of gas bubbles in tissues. At the average HIFU intensities, a bubble vibrates firmly in an acoustic field while absorbs and radiates energy to the surrounding, called stable cavitation.

However, when the acoustic intensity increases, the bubble vibrations become significantly nonlinear and lead to violent collapse, known as inertial cavitation. Inertial cavitation stimulates the micro jets, shock wave, and highly elevated local heat that may reach thousands of degrees Kelvin. The free radicals produced in these temperatures can cause mechanical cell destruction and even melting the solid cells and tissues.

If controlled, highly localized hyperthermia is the desired outcome, then most investigators may argue that cavitation is to be avoided because it has typically leads to unpredictable thermal results. Several authors have observed irregular lesions and collateral damage outside the focal zone when uncontrolled cavitation occurred during insonation [24-27]. These studies all contain unambiguous statements recommending actively avoiding cavitation when the therapeutic goal is the controlled localized heating.

Although cavitation-related enhanced heating is observed in some of the preceding studies [22,23], the observation of enhanced heating due to bubble activity deserves closer attention. A pressure threshold for enhanced heating of about 5.3 MPa at 1 MHz is reported [22].

The goal of this study is the development of a computational tool for HIFU ablation therapy to assure safety of the patient and effectiveness of the treatment. The proposed model could simulate the non-linear wave propagation from the source and distribution of excitation through tissue layers. The performance of phased array HIFU can be improved in the treatment planning. Numerical simulation represents a useful approach to predicting the pressure and temperature distributions and, consequently, gauging the safety and effectiveness of HIFU devices.

## Nomenclature

| | |
|---|---|
| $B$ | Nonlinearity parameter |
| $C$ | Speed of sound (m/s) |
| $C_P$ | Heat capacity at constant pressure (J/kg.K) |
| $f$ | Frequency (Hz) |
| $I$ | Intensity (W/m$^2$) |
| $K$ | Thermal conductivity (W/m.K) |
| $n_k$ | Wave direction |
| $P$ | Pressure (Pa) |
| $P_b$ | Background pressure (Pa) |
| $P_t$ | Total pressure (Pa) |
| $q_d$ | Dipole source (N/m$^3$) |
| $Q_m$ | Monopole source (1/s$^2$) |
| $Q_{\text{met}}$ | Metabolic heat source (W/m$^3$) |
| $T$ | Temperature (K) |
| $T_b$ | Arterial blood temperature (K) |
| $\alpha$ | Attenuation coefficient ($N_P$/m) |
| $\gamma$ | Ratio of specific heats |
| $\delta$ | Diffusivity of sound (m$^2$/s) |
| $\lambda$ | Wave length (m) |
| $\mu$ | Dynamic viscosity (Pa.s) |
| $\mu_B$ | Bulk viscosity (Pa.s) |
| $\rho$ | Density (kg/m$^3$) |
| $\omega$ | Angular frequency (rad/s) |

### *Index*

| | |
|---|---|
| b | Blood |
| Max | Maximum |
| Min | Minimum |

## References

1. Zhou, M., Chen, J.Y., Tang, L.D., Chen, W.Z., and Wang, Z.B. "Ultrasound-guided high-intensity focused ultrasound ablation for adenomyosis: the clinical experience of a single center", *Fertil. Steril.*, **95**(3), pp. 900-905 (2011).
2. Leslie, T.A. and Kennedy, J.E. "High intensity focused ultrasound in the treatment of abdominal and gynecological diseases", *Int. J. Hyperthermia.*, **23**, pp. 173-182 (2007).
3. Bailey, M.R., Khokhlova, V.A., Sapozhnikov, O.A., Kargl, S.G., and Crum, L.A. "Physical mechanisms of the therapeutic effect of ultrasound", *Acoust. Phys.*, **49**(4), pp. 369-388 (2003).
4. Hynynen, K., Chung, A.H., Colucci, V., and Jolesz, F.A. "Potential adverse effects of high-intensity focused ultrasound exposure on blood vessels in vivo", *Ultrasound in Medicine & Biology*, **22.2**, pp. 193-201 (1996).
5. Bjorno, L. "Forty years of nonlinear ultrasound", *Ultrasonics*, **40**, pp. 11-17 (2002).
6. Hallaj, I.M., and Cleveland, R.O. "FDTD simulation of finite-amplitude pressure and temperature fields for biomedical ultrasound", *J. Acoust. Soc. Am.*, **105**(5), pp. L7-12 (1999).
7. Curra, F.P., Mourad, P.D., Khokhlova, V.A., Cleveland, R.O., and Crum, L. A. "Numerical simulations of heating patterns and tissue temperature response due to high-intensity focused ultrasound", *IEEE Trans. Ultrason. Ferroelectr. Freq. Control.*, **47**(4), pp. 1077-1089 (2000).
8. Hariharan, P., Myers, M.R., and Banerjee, R.K. "HIFU procedures at moderate intensities effect of large blood vessels", *Phys. Med. Biol.*, **52**(12), pp. 3493-513 (2007).
9. Okita, K., Ono, K., Takagi, S., and Matsumoto, Y. "Development of high intensity focused ultrasound simulator for large-scale computing", *Int. J. Numer. Methods. Fluids.*, **65**(1-3), pp. 43-66 (2011).
10. Wong, S.H., Kupnik, M., Butts-Pauly, K., and Khuri-Yakub, B.T. "P1B-10 advantages of capacitive micromachined ultrasonics transducers (CMUTs) for high intensity focused ultrasound (HIFU)", *IEEE Int. Ultrason. Symp.* (2007).
11. Hamilton, M.F., Morfey, C.L., and Blackstock, D.T. "Model equations", *Nonlinear Acoustics*, **427**, San Diego: Academic press. (1998).
12. Soneson, J.E. "A parametric study of error in the parabolic approximation of focused axisymmetric ultrasound beams", *J. E. Soneson, J. Acoust. Soc. Am.*, **131**(6), pp. EL481-486 (2012).
13. Tjo, J.N. and Vefring, E.H. "Effects of focusing on the nonlinear interaction between two collinear finite amplitude sound beams", *J. Acoust. Soc. Am.*, **89**(3), pp. 1017-1027 (1991).
14. Tavakkoli, J., Cathignol, D., Souchon, R., and Sapozhnikov, O.A. "Modeling of pulsed finite-amplitude focused sound beams in time domain", *J. Acoust. Soc. Am.*, **104**(4), pp. 2061-2072 (1998).
15. Yuldashev, P.V. and Khokhlova, V.A. "Simulation of three-dimensional nonlinear fields of ultrasound therapeutic arrays", *Acoust. Phys.*, **57**(3), pp. 334-343 (2011).
16. Wojcik, G., Mould, J., Abboud, N., Ostromogilsky, M., and Vaughan, D. "Nonlinear modeling of therapeutic ultrasound", In *Ultrasonics Symposium*, Proceedings., IEEE, **2**, pp. 1617-1622 (1995).
17. Khokhlova, V.A., Bessonova, O.V., Soneson, J.E., Canney, M.S., Bailey, M.R., and Crum, L.A. "Bandwidth limitations in characterization of high intensity

focused ultrasound fields in the presence of shocks", In K. Hynynen and J. Souquet Eds., *AIP Conference Proceedings*, **1215**(1), pp. 363-366, AIP (2010).

18. Joshua E. Soneson "A user-friendly software package for HIFU simulation", *AIP Conference Proceedings*, Emad S. Ebbini, Ed., **1113**(1), AIP (2009).

19. Solovchuk, M., Sheu, T.W., and Thiriet, M. "Simulation of nonlinear Westervelt equation for the investigation of acoustic streaming and nonlinear propagation effects", *J. Acoust. Soc. Am.*, **134**(5), pp. 3931-3942 (2013).

20. Sapareto, S.A. and Dewey, W.C. "Thermal dose determination in cancer therapy", *Int. J. Radiat. Oncol. Biol. Phys.*, **10**(6), pp. 787-800 (1984).

21. Karaböce, B. and Durmuş, H.O. "Visual investigation of heating effect in liver and lung induced by a HIFU transducer", *Phys. Procedia.*, **70**, pp. 1225-1228 (2015).

22. Hynynen, K. "The threshold for thermally significant cavitation in dog's thigh muscle in vivo", *Ultrasound in Medicine* & *Biology*, **17**(2), pp. 157-169 (1991).

23. Clarke, R.L. and Ter Haar, G.R. "Temperature rise recorded during lesion formation by high-intensity focused ultrasound", *Ultrasound in Medicine* & *Biology*, **23**(2), pp. 299-306 (1997).

24. Chapelon, J.Y., Prat, F., Delon, C., Margonari, J., Gelet, A., and Blanc, E. "Effects of cavitation in the high intensity therapeutic ultrasound", In *Ultrasonics Symposium, Proceedings, IEEE 1991*, pp. 1357-1360 (1991).

25. Chapelon, J.Y., Dupenloup, F., Cohen, H., and Lenz, P. "Reduction of cavitation using pseudorandom signals [therapeutic US]", *IEEE Transactions on Ultrasonics, Ferroelectrics, and Frequency Control*, **43**(4), pp. 623-625 (1996).

26. Chapelon, J.Y., Cathignol, D., Cain, C., Ebbini, E., Kluiwstra, J.U., Sapozhnikov, O.A., Fleury, G., Berriet, R., Chupin, L., and Guey, J.L. "New piezoelectric transducers for therapeutic ultrasound", *Ultrasound in Medicine* & *Biology*, **26**(1), pp. 153-159 (2000).

27. Sibille, A., Prat, F., Chapelon, J.Y., et al. "Characterization of extracorporeal ablation of normal and tumor-bearing liver tissue by high intensity focused ultrasound", *Ultrasound in Medicine* & *Biology*, **19**(9), pp. 803-813 (1993).

## Biographies

**Samaneh Haddadi** received her BS degree in Mechanical Engineering in 2005 from University of Tehran, Tehran, Iran and completed the requirements for MS degree in Mechanical Engineering in 2008 from Sharif University of Technology, Tehran, Iran. She has been studying to get PhD in Mechanical Engineering from 2011 in Sharif University of Technology. Her research interests are Ultrasonics and Bioengineering.

**Mohammad Taghi Ahmadian** received his BS and MS degrees in Physics in 1972 from Shiraz University, Shiraz, Iran and completed the requirements for BS and MS degrees in Mechanical Engineering in 1980 from University of Kansas in Lawrence. At the same time, while getting his master degree, he completed his PhD in Physics and PhD in Mechanical Engineering in 1981 and 1986, respectively, from University of Kansas. He started working as an Assistant Professor in Sharif university of Technology from 1989; at present, he is a Professor in the School of Mechanical Engineering in Sharif University of Technology, Tehran.